EIGHTH INTERNATIONAL SYMPOSIUM ON APPLICATIONS OF LASER TECHNIQUES TO FLUID MECHANICS
July 8 - 11, 1996, Lisbon, Portugal

FLOW OF SHEAR-THINNING FLUIDS AROUND A CYLINDER: VORTEX SHEDDING AND DRAG CHARACTERISTICS

P. M. Coelho, F. T. Pinho, A. H. Rodrigues

Departamento de Engenharia Mecânica e Gestão Industrial
Faculdade de Engenharia, Rua dos Bragas, 4099 Porto Codex, Portugal

ABSTRACT

Measurements of the vortex shedding frequency in the wake of a cylinder and of the pressure profile around its surface were carried out for various elastic, shear-thinning fluids and compared with those of Newtonian fluids. The results obtained so far show that the normalised vortex shedding frequency increases with polymer concentration for flows pertaining to the subcritical regime. This effect is due to the thinning of the boundary layer associated with a shear-thinning viscous behaviour, whereas the elasticity of the fluids was found to have the opposite effect.

The form drag coefficient was calculated from the measured pressure profiles at the surface of the cylinder, and it was found that its reduction could be accounted for by both the shear-thinning and the fluid elasticity.

1. INTRODUCTION

The flow around a cylinder is a basic flow, whose knowledge is fundamental to a comprehensive understanding of the more complex flow around rod bundles, this one of particular relevance in tube-shell heat exchangers. Many engineering processes of the food, detergent and allied industries, amongst others, involve heat transfer with non-Newtonian fluids of low viscosity, but the information pertaining to these flows is scarce in the literature. This is the motivation for this work, which starts by investigating the hydrodynamics of the cross flow of shear-thinning fluids around a cylinder.

As far as Newtonian fluids are concerned, there has been extensive work due to the relevance of the flow for similar purposes and in other practical situations, such as in hydraulics, and two important references on the subject are the paper of Cantwell and Coles (1983) and the recent review of Telionis *et al.* (1992). However, for non-Newtonian fluids most of the work is theoretical and numerical, and is mainly concerned with creeping flows.

Shah *et al.* (1962) were among the first to experimentally investigate cross flows of non-Newtonian fluids around cylinders, up to Reynolds numbers as high as 12000. They found that the circumferential pressure profile on the cylinder laminar-boundary layer, with shear-thinning, elastic aqueous solutions of CMC, were independent of the power law of the viscosity consistency (k) and power (n) indices.

The measurements of the hydrodynamic and heat transfer characteristics of elastic fluids of constant viscosity of James and Acosta (1970) and James and Gupta (1971) were limited to lower maximum Reynolds numbers of 50 and 200, respectively. Both works reported that, at the high Reynolds number range, the drag coefficient and Nusselt number were independent of the Reynolds number but not of the Weissenberg number.

On the vortex shedding phenomena from a circular cylinder, it is important to refer the work of Gerrard (1966), who proposed a mechanism to explain its hydrodynamic characteristics based on two characteristic lengths, the formation and the diffusion lengths. According to Bloor (1964), the formation region (l_f) goes from the rear stagnation point up to the location where fluid from outside the wake first crosses the flow symmetry plane, as it is entrained by the opposite shear layer. The second characteristic length, which he termed the diffusion length (L), is the thickness of the free shear layer measured at the end of the formation region. Thus, the Strouhal number varies inversely with l_f and L.

In this work, results of measurements of the static pressure around the cylinder and of the frequency of the vortices shed in the wake of the cylinder, for various aqueous polymer solutions and two Newtonian fluids, are presented and discussed.

The next section describes the rig, the instrumentation and the corresponding uncertainties. Then, the rheological characteristics of the fluids are presented, before the results are shown and discussed. A summary of the main conclusions closes the paper.

2. EXPERIMENTAL FACILITY

The measurements were carried out in a water tunnel, shown schematically in figure 1, which had a 6 to 1 contraction before a transparent test section 197 mm high and 120 mm wide. The cylinder had a diameter of 19.7 mm, leading to a blockage of 10%, an aspect ratio of 6:1 and it was located 7 diameters downstream of the test section entrance. In order to reduce vibrations the test section and the settling chamber were isolated from the rest of the rig by means of flexible rubber pipes. The maximum mean velocity in the test section was about 2 m/s, corresponding to a maximum flow rate of 170 m^3/h, regardless of the fluid. The mean velocity profile at the test section inlet, outside the wall boundary layers, was cons-

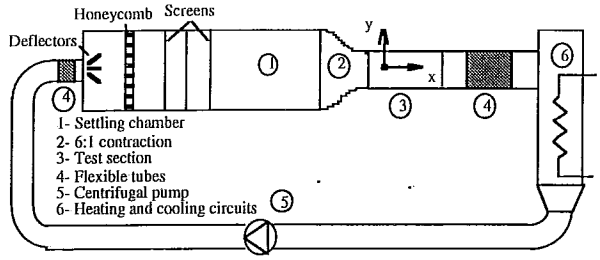

Figure 1 - Schematic representation of the water tunnel.

tant to within 1% and the free stream turbulence was equal to 3.9% at a flow rate of 85 m^3/h.

In order to reduce the level of free stream turbulence, a long settling chamber with a large cross section would have been required, thus increasing enormously the volume of the rig. Budgetary constraint also imposed the purchase of a centrifugal pump, known to cause a much more intense mechanical degradation than that of a volumetric pump, Pinho and Whitelaw (1991).

The intense degradation of the polymer molecules requires frequent fluid substitution, of about 6 to 20 h, depending on the fluid resistance. Therefore, the volume of the rig of around 450 l, was a compromise between a reasonable flow condition at the test section, an affordable water tunnel and an easy and not to expensive fluid substitution procedure.

The heat exchanger, where tap water was the coolant and electrical resistances provided the heating, allowed the temperature to be maintained at 25°C during the whole test, with a variation never exceeding 0.5°C.

A diode fibre-optic laser-Doppler system from INVENT, model DFLDA, was used for the velocity measurements in the wake of the cylinder. A full description of this anemometer can be found in Stieglmeier and Tropea (1992). The S30 optical probe, with a 120 mm focusing lens, was used and the LDA main characteristics are listed in table 1. The output of the avalanche photodiode was processed by a 1990C TSI counter with 2^5 cycles using the single measurements per burst mode and the validation criteria set to 1% comparison. The large number of cycles was possible since, according to Tropea (1993), the frequency shift adds N_{sh} fringes to the measuring volume equivalent in number to:

$$N_{sh}=\frac{f_{sh}\, d_{mcv}}{U_P} \qquad (1)$$

where f_{sh} is the shift frequency and d_{mcv}/U_p is the residence time of the particle (d_{mcv}- control volume diameter; U_P- particle velocity). The frequency information from the counter was then sent to a computer via a DOSTEK 1400A interface card for further statistical and numerical analysis. In order to minimise velocity bias effects the data was acquired at a predefined frequency, rather than on the basis of the arrival data rate, which was higher than the timer frequency.

The high data rate signal measured downstream of the cylinder was processed by the FFT routines included in the software from DOSTEK to output the vortex shedding frequency. Note that for these measurements, the acquisition frequency was always at least 5 times higher than the frequency of the shedding. Figure 2 is a typical example of the measured power spectral density distribution (PSD) as a function of the frequency, plotted in log-log coordinates.

Table 1- Main characteristics of the Laser Doppler anemometer

Laser Wavelength	827 nm
Laser power	100 mW
Measured half angle of beams in air	3.68°
Measuring volume size in water (e^{-2} intensity)	
minor axis	37 μm
major axis	550 μm
Fringe spacing	6.44 μm
Frequency shift	2.0 MHz

The velocimeter was mounted on a milling table with movement in the three orthogonal directions and the estimated maximum uncertainty of the mean velocity and frequency measurements, at a 95% confidence level was always better than 1.5%, calculated following Durst *et al.* (1981). As far as the positional uncertainty is concerned, it was of ± 20 μm in the x-z horizontal plane and of ± 10 μm in the vertical direction.

The pressure measurements were carried out with three different P305D Validyne differential pressure transducers, diaphragm numbers 30, 24 and 20 with full scale values of 880, 200 and 80 mm H_2O, respectively.

One pressure tap of 0.3 mm in diameter was drilled on the surface of the cylinder, which could rotate about its axis. The small size of the tap meant that for the more viscous fluids (0.4% CMC and 0.6% Tylose), the response time was slow, of about two minutes, in spite of the fact that the connecting tubes were filled with water.

The pressure transducers were connected to a 386 PC via a data acquisition Metrabyte board DAS8 and a Metrabyte ISO4 multiplexer board. For each angular location a sample size of 2000 measurements was taken and the statistical quantities were calculated by purpose-built software, with an estimated overall uncertainty of 4.3%, 0.8% and 1.2% for the pressure transducers number 30, 24 and 20, respectively.

3. FLUIDS CHARACTERISTICS

Two different polymers, of high and low molecular weights, were dissolved in water to manufacture elastic

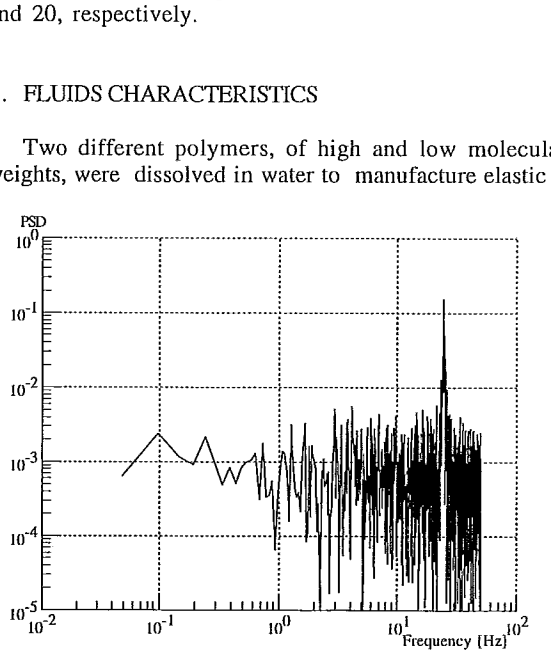

Figure 2 - PSD versus frequency for 0.6% Tylose and Re= 848.

and weakly elastic shear-thinning fluids, respectively, and the results compared to those of two Newtonian fluids of different viscosity.

The weakly elastic fluids, Pereira and Pinho (1994), were aqueous solutions of 0.2, 0.3, 0.4 and 0.6% by weight concentration of a methyl hydroxyethyl cellulose called Tylose, grade MH 10 000K from Hoechst, which had a molecular weight of 6 000 kg/kmol. The more elastic aqueous solutions were manufactured from carboxy methyl cellulose sodium salt, (CMC) grade 7H4C from Hercules, which had a molecular weight of 300 000 kg/kmol, at concentrations of 0.1, 0.2, 0.3 and 0.4% by weight. A biocide, Kathon LXE 1.5% from Rohm & Haas, at a concentration of 0.02% by weight, was added to all solutions of CMC, to prevent bacteriological growth and degradation.

The Newtonian fluids were water and a mixture of 40% water and 60% glycerin with a viscosity of 0.0073 Pa.s.

The densities and refractive indices of all non-Newtonian fluids were unchanged from those of water (ρ=998 kg/m^3, n=1.333) at 25°C, whereas for the glycerin-water mixture they were of 1148 kg/m^3 and 1.409, respectively. Figure 3 shows the viscosity of all non-Newtonian solutions as a function of the shear rate.

An assessment of some elastic material functions for the Tylose solutions is given in Pereira and Pinho (1994) and for the CMC solutions in Escudier *et al.* (1996).

4. RESULTS AND DISCUSSION

The minimisation of blockage corrections in wind and water tunnels usually requires the use of large test sections. In spite of being an old issue, e.g. Allen and Vicenti (1944) as quoted by Roshko (1961), Maskell (1963) and Farrel *et al.* (1977), there is not yet a widely accepted procedure for correcting for blockage effects. According to West and Apelt (1982), for a 10% blockage as in here the usual correction leads to a poorer drag coefficient (C_d), and the correction of the Reynolds number increases its value by at most 4%. Therefore, and considering also the unknown effects of the non-Newtonian characteristics of the fluids on what concerns this issue, no blockage corrections will be applied to the present experimental data.

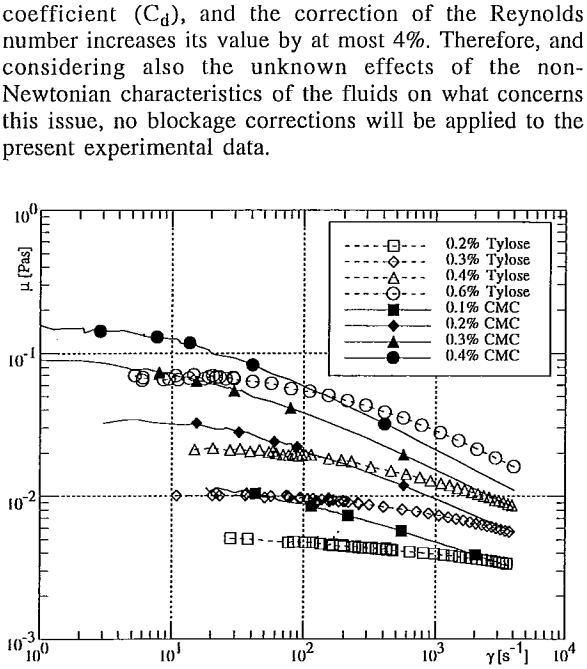

Figure 3 - Viscosity versus shear rate at 25°C.

In non-Newtonian fluid mechanics the pertinent issue of the adequate viscosity for normalisation arises. In simple flows, such as in a turbulent boundary layer over a flat plate, the argument for selecting the wall viscosity is relatively straightforward, but in more complex flows, such as this one, the decision is not so easy.

Selecting a proper viscosity is equivalent to selecting a characteristic shear rate that dominates the main flow hydrodynamic features. One of the advantages of dimensional analysis is the possibility it gives of comparing similar flows with different fluids and sizes without knowing *a priori* their detailed flow characteristics. This suggests that one should base the characteristic shear rate on integral, general quantities and geometrical dimensions, rather than on measured local quantities.

The obvious selection for the cylinder cross flow is the ratio of the free stream velocity to the cylinder radius (U_∞/R), but the work of Gerrard (1966) on Newtonian cylinder flows has shown that the important flow characteristics downstream of the cylinder depend of the shear layer thickness at the end of the formation region. Then, a more appropriate characteristic viscosity could be somehow related to this shear rate, but this requires the detailed knowledge of the flow field.

If the issue is irrelevant for Newtonian flows, it becomes important once the viscosity varies. In this work, the contradictions between these two approaches will come to light and a first attempt to solve it will be proposed and discussed.

Initially, a Reynolds number of

$$Re=\frac{\rho U_\infty D}{\mu_{ch}} \qquad (2)$$

where ρ, U_∞, D and μ_{ch} are the fluid density, freestream mean velocity, cylinder diameter and characteristic viscosity, will be defined with the characteristic shear rate set as the ratio of the free stream mean velocity to the cylinder radius. Later on, an alternative based on an estimate of local shear rates at the boundary layer will be discussed.

Figure 4 shows a plot of the Strouhal number ($Sr=f.D/U_\infty$), where f stands for the vortex shedding frequency, as a function of the Reynolds number for all the solutions. The broken line represents the Newtonian data of Norberg (1994) without blockage or end plate effects. The fact that our measurements with Newtonian fluids are below those of Norberg, for Reynolds numbers under 5300, can be explained by the influence of the boundary layer at the tunnel side walls on the mechanism of vortex shedding, according to Gerich and Eckelmann (1982) and Stäger and Eckelmann (1991). To reduce this effect, end plates on the cylinder edges are commonly use, thus replacing the boundary layer on the tunnel wall by a thinner boundary layer on the end plates surface. In the present case, since the cylinder is located at 7 cylinder diameters from the entrance of the test section the tunnel walls behave roughly like end plates, except that the flow at the connection between the test section and the contraction is different from that at the leading edge of a real end plate. .

According to Stäger and Eckelmann (1991) the end plates reduce the affected area to the edges of the cylinder, a region that decreases as the Reynolds number increases. Since the aspect ratio of the current experiments is not

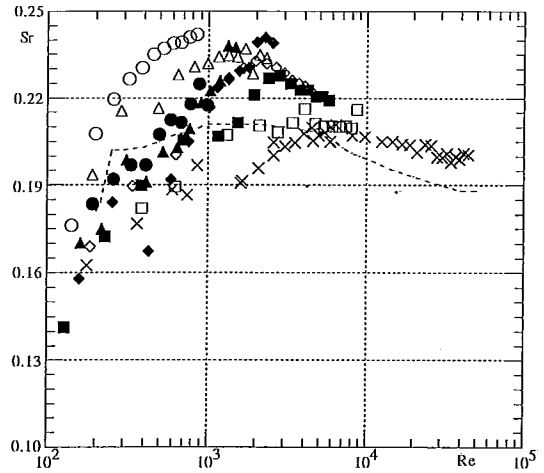

Figure 4 - Strouhal number versus Reynolds number for all solutions. □ 0.2% Tylose; ◊ 0.3% Tylose; Δ 0.4% Tylose; O 0.6% Tylose;■ 0.1% CMC; ◆ 0.2% CMC; ▲ 0.3% CMC; ● 0.4% CMC;X Newtonian; ---- Norberg (1994)

very high, at low Reynolds number flows the end plate effect can span all the cylinder length. In the affected region, the shedding frequency is always smaller than that in the unaffected region, represented by the Norberg values in figure 4. According to Stäger and Eckelmann (1991), for an end plate with dimensions similar to ours the Reynolds number above which the end plate effects cease to exist is approximately 3 000, but since truly end plates were not used, it is reasonable to expect that this critical Reynolds number value is different from 3 000. The measured Strouhal number values start to be higher than those of Norberg (1994), for Reynolds numbers above 5 300, therefore one may conclude that above this number the end plate effects become negligible.

At the high Reynolds number range, higher Strouhal number values relative to those of Norberg (1994), at the high Reynolds number range, were expected because they are the outcome of the blockage effect, following West and Apelt (1982). According to them, a 10% blockage at a Reynolds number of 10^4 corresponds to an increase in the Strouhal value of 0.005, whereas our data is 0.015 higher than the situation of no blockage. At this Reynolds number range the aspect ratio does not affect the Strouhal number (negligible end plate effects according to West and Apelt, 1982), so the extra difference between ours and Norberg's data can only be explained by the higher freestream turbulence intensity.

The values of the Strouhal number for the non-Newtonian fluids are well above those for Newtonian fluids, but they follow the same pattern, i.e. the Strouhal number increases first at low Reynolds numbers, reaching a maximum of 0.24, decreasing afterwards towards a constant value of around 0.2 at higher Reynolds numbers. So, the major difference in the value of the Strouhal number is at the low Reynolds number range, with the non-Newtonian fluids exhibiting a higher frequency of vortex shedding, which also increases with the polymer concentration. Note, however, that this Reynolds number effect may not exist, because it depends of the definition of the viscosity, as will be shown later.

The formation length, the boundary layer and shear layer thicknesses for these non-Newtonian fluid flows were not measured yet, therefore we are still unable to confirm the following tentative theory. According to Gerrard (1966), the formation length mainly depends of the turbulent entrainment by the shear layer, of fluid coming from the opposite shear layer, most of which bears opposite signed vorticity. This latter fluid will influence the vortex strength, and consequently the flow that goes into the formation region (reverse flow), thus reducing its length, i.e., a smaller reversed flow will induce a shorter formation region. This argument means that the formation length should increase, and according to Roshko (1954 b) as quoted by Gerrard (1966) the frequency decrease, the higher the capability of the fluid to delay the transition to turbulence, i.e., the higher the concentration of polymer.

The observed tendency is the opposite, so, still following Gerrard's (1966) theory, it must be the other characteristic length (the diffusion length) which is playing here the most important role, even when the shear layers are completely laminar (Reynolds numbers below 700 for flows with low free-stream turbulence, according to Gerrard, 1978). Serth and Kiser (1967) have shown that the boundary layer thickness in the flow over a flat plate is thinner with shear-thinning fluids than with constant viscosity fluids. The same effect is bound to occur in the flow around a cylinder, i.e. the shear layer will be thinner for higher polymer concentrations, which is the same as saying that the diffusion length will be thinner and the Strouhal number higher. The Tylose solutions emphasize this effect: as the polymer concentration is raised, the shear-thinning is intensified, thinning the boundary and shear layers and increasing the shedding frequency.

The decrease of the Strouhal number at higher Reynolds numbers could be explained by the same mechanism acting in the opposite way; shear layers (diffusion lengths) are thickening by virtue of the increased flow turbulence and the shedding frequency decreases. Quoting Gerrard (1966) "...when the layer is diffused it will take longer for a sufficient concentration of vorticity (of opposite sign) to be carried across the wake and initiate shedding. So we expect the shedding frequency to decrease as the diffusion length L increases.". Obviously this effect should be stronger than the attendant reduction in the formation length in order to justify the Strouhal number decrease.

The behaviour of the weakly elastic Tylose solutions agrees with this theory, but the data pertaining to the more elastic aqueous solutions of CMC do not confirm it so well. Although an increased Strouhal number is still observed, its systematic increase with the polymer concentration is not so intense as with the Tylose solutions, for a similar progression of the power law index (n).This different behaviour of the CMC solutions will be confirmed later by the drag coefficient measurements and the reason for it could be attributed to elasticity effects in the boundary and shear layers.

Metzner and Astarita (1967) have shown that by virtue of the great resistance which the elastic fluids manifest when they are subjected to sudden changes in the flow and consequently to high shear rates, they develop a thicker boundary layer, that extends to the forward stagnation point in the case of flow around bodies. This

forces the potencial-flow velocity field outside the boundary layer to adjust to a larger radius of curvature. The higher the elasticity of the fluid, the more prone will be the fluid to this effect.

There are many demonstrations of the elasticity of CMC solutions, as in the experiments of Pinho and Whitelaw (1990), especially in the presence of turbulence. The experimental work on the laminar flow of elastic and inelastic non-Newtonian fluids around spheres of Acharya *et al.* (1976 a and b) and Adachi *et al.* (1977/78) have clearly demonstrated that on account of fluid elasticity the separation bubble behind the sphere was shorter than for inelastic fluids, and that there was an upstream shift of the streamlines, in agreement with the theory put forward by Metzner and Astarita (1967). As far as the drag coefficients were concerned, the elasticity was seen to reduce these values relative to those pertaining to inelastic fluids.

The relative constancy of the Strouhal number with polymer concentration for the CMC solutions can then be related to the opposite effects of the elasticity and shear-thinning upon the shear layer thickness, and consequently upon the diffusion length. The recent rheological measurements of Escudier (1996) have shown that to higher concentrations of CMC correspond higher intensities of shear-thinning and of elastic quantities, so their effects may somehow cancel each other.

Whereas the increased Strouhal number of non-Newtonian fluids is independent of the definition of the characteristic viscosity and is truly a non-Newtonian effect, the shift in the curves plotted in figure 4 to lower Reynolds number, depends on that choice.

If the arguments put forward by Gerrard (1966) on the role of the diffusion length are accepted, which we did to explain the increased shedding frequency, then the characteristic shear rate should be somehow related to the diffusion length, which is to say to the shear layer thickness in the formation region. However this quantity was not measured and had to be estimated. In addition, a method which does not require an *a priori* knowledge of the detailed flow field should be preferred.

In this attempt to quantify more realistically the shear rates encountered by the fluids following a general procedure, the choice was the well-know integral method of Thwaites based on Newtonian fluids, as explained by White (1991). According to this work, the value of the shear rate over a circular cylinder, at an angle of 70° from the forward stagnation point, represents reasonably well in order of magnitude the shear rates near the separation for the case of a laminar boundary layer flow over a circular cylinder.

The Thwaites method was used in conjunction with Hiemenz potential flow velocity field to calculate the wall shear stress at 70° (using equations 4-132 to 4-139 of White 1991) and yielded values of the characteristic shear rate 13 to 50 times higher than U_∞ / R, corresponding to the lowest and highest flow rates tested. The order of magnitude of those shear rates also compared well with values calculated in a set of numerical simulations that were performed for the same flow around a cylinder, assuming symmetry of the flow. These calculations were carried out using a finite- volume based code, described by Oliveira (1992), with CDS and LUDS

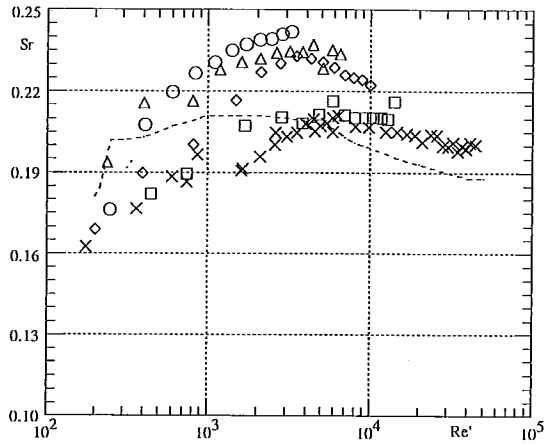

Figure 5 - Strouhal number versus Reynolds number calculated with the characteristic shear rate based on Thwaites method. □ 0.2% Tylose; ◊ 0.3% Tylose; Δ 0.4% Tylose; O 0.6% Tylose;X Newtonian; ---- Norberg (1994)

as differencing schemes for diffusion and convection, respectively.

Using these characteristic shear rates a new Reynolds number designated by Re' was defined, and the Strouhal number data pertaining to the negligibly elastic Tylose solutions of figure 4, were plotted again in figure 5.

With this new Reynolds number the Strouhal number curves moved closer to each other, with its maximum value for the 0.3%, 0.4% and 0.6% Tylose solutions, occurring at basically the same Reynolds number, and with all the data spanning now roughly the same range of Reynolds numbers. It is now necessary to measure the velocities in the boundary and shear layers in order to quantify the real shear rate and definitely validate and/or improve this procedure, a task which will be carried out in the near future.

In figure 6 a typical non-dimensional pressure distributions around the cylinder is shown. By definition, the pressure coefficient is 1 in the forward stagnation point, it decreases until the minimum pressure coefficient (C_{pm}) at around 70° to 73°, and increases again to an approximately constant value (C_{pb}) at the back of the cylinder. The tunnel static pressure was calculated from the total pressure measured at the forward stagnation point of the cylinder, and the approach velocity measured by LDV. Small differences in the symmetry of the pressure distribution around the cylinder were found in the range 70°-100°, never exceeding 7% for the Tylose solutions and 3% for CMC and Newtonians solutions. A small perturbation in the oncoming flow could be responsible for this behaviour.

The pressure distribution around the cylinder was processed to evaluate various quantities: its integration all around the cylinder with a Newton-Cotes formula quantified the form drag coefficient (C_d), the mean value of the pressure coefficient between 120° and 240° degrees defined the base pressure coefficient (C_{pb}), the minimum pressure value quantified the minimum pressure coefficient (C_{pm}), and the approximate location of the beginning of the wake region (θ_w) was defined as suggested by

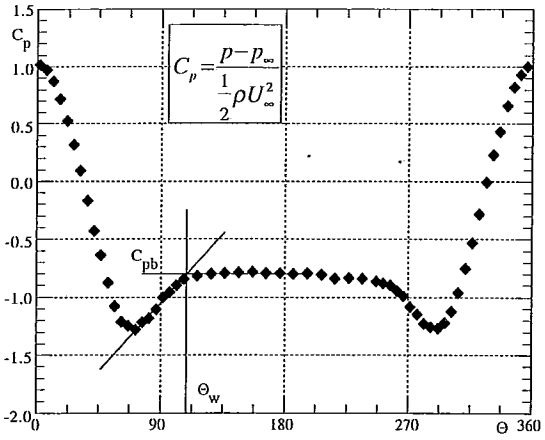

Figure 6- Typical non-dimensional pressure distributions around the cylinder for a Reynolds number (Re≈ 800).◆ 0.2% CMC

Niemann, according to Guven *et al.* (1980) (see sketch on figure 6). The pressure rise coefficient (C_{pb}-C_{pm}) is a measure of the pressure rise sustained by the boundary layer prior to separation and it was also calculated. It is an important parameter, because it is insensitive to the blockage ratio, as explained by Farell *et al.* (1977).

The form drag coefficient is shown in figure 7 as a function of the two Reynolds numbers defined in this paper, with the full line representing the Newtonian values of C_d measured by Wieselsberger, as presented in Roshko (1961). Figure 8 shows the pressure rise coefficient for the same solutions and in figure 9, values of the wake angle calculated as the averaged value of the wake angles from the two sides of the cylinder following the procedure outlined above, are presented.

The Newtonian curve for the C_d pertains to the total drag coefficient whereas data measured in this work only refers to the pressure contribution. The range of Reynolds numbers covered by the current measurements is not so extensive as that pertaining to the data from the literature, therefore the typical U-shaped curve is not observed clearly for all the fluids. Bearing this in mind and that the data in the figure was calculated rather than measured, it is not surprising the degree of scatter observed in it.

The Tylose solutions show a reduction of the minimum form drag coefficient with polymer concentration. The shift of the curves to lower Reynolds numbers in figure 7a) is associated with using U_∞/R as the characteristic shear rate for the calculation of viscosity, and it disappears if the alternative Reynolds number based on Thwaites method is used (figure 7b).

The aqueous solution of 0.2% Tylose behaves similarly to the Newtonian fluids, not just in the shedding frequency but also in the C_d, which is not surprising since it is the least shear thinning and elastic of all non-Newtonian fluids.

As far as the CMC solutions are concerned, they exhibit a lower form drag than the correspondingly similar shear-thinning weakly elastic solutions, as was also observed for the total drag in the sphere flows of Adachi *et al.* and Acharya *et al.*, and in agreement with the reported tendencies associated with elastic behaviour, namely a delayed flow separation.

For Reynolds numbers smaller than 700, the solutions of 0.6% Tylose and 0.4% CMC have a fairly constant C_d, but lower than the Wieselsberger Newtonian curve, a result that contradicts the measurements of James and Gupta (1971). One possible explanation for this discrepancy is that we have measured the pressure drag of elastic shear-thinning fluids, whereas James and Gupta measured the total drag with elastic fluids of constant viscosity. Achenbach (1971) has demonstrated that in the subcritical regime, and for Reynolds numbers above $2x10^4$, the friction forces contribute with less than 2% to the total flow resistance. However, we could not find any reference in the literature to the contribution of frictional drag for lower Reynolds numbers, but it is reasonable to expect that here it will be higher, because the separation occurred later, at an angle above 100° for Reynolds number below 1 000 (figure 9), and also because the velocity gradients at the wall are higher on account of the pseudo-plasticity of the fluids, Serth and Kiser (1967). Another possible reason for this can be the end plate effects, which according to Norberg (1994) measurements substantially increases the base pressure coefficient (C_{pb}) thus decreasing the drag coefficient (C_d).

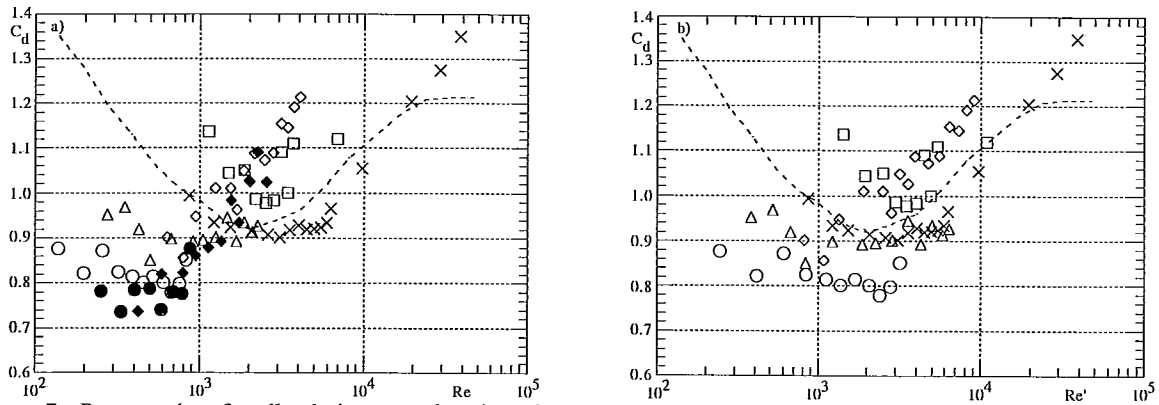

Figure 7 - Pressure drag for all solutions as a function of the two different Reynolds numbers: a) Re b) Re'. □ 0.2% Tylose; ◊ 0.3% Tylose; Δ 0.4% Tylose; O 0.6% Tylose;◆ 0.2% CMC; ● 0.4% CMC; X Newtonian; ---- Wieselsberger.

The pressure rise coefficient (C_{pb}-C_{pm}) shown in figure 8 changes slowly with the Reynolds number for each fluid, therefore the Reynolds number definition is not so important in this plot. One can see in the figure that the more elastic solutions, represented by the CMC, exhibit higher pressure rises before separation. In this region the polymer molecules are being subjected to a compression and it is known (Bird *et al*, 1987) that elastic fluids resist more to the normal deformations, so they can sustain a larger pressure rise. If this is true, then the more concentrated Tylose solutions are exhibiting some elasticity as their pressure rise coefficient are above those of Newtonian fluids, but not so intense as for the CMC solutions. This is a speculative argument, but Pereira and Pinho (1994) have found out that all solutions of Tylose exhibited some elongational elasticity effects under the presence of turbulence, in spite of their low molecular weight, and in this flow the free-stream turbulence is in excess of 3%.

With a fairly constant pressure rise with the Reynolds number, especially with the polymeric solutions, the wake angle should not vary as much as depicted in figure 9.

In the subcritical regime the wake angle should be less than 90°, but as shown in figure 9 for the lower Reynolds numbers the separation occurs at more than 115°, decreasing to less than 85° as the Reynolds number increases above 10 000, a result also confirmed by flow visualisation experiments using dyes.

There are two possible causes for this: first, the end plate effect, which decreases as the Reynolds number increases and is thus responsible for an earlier separation and larger drag. Secondly, the turbulence of the free-stream flow was found to increase from about 3% at the higher Reynolds numbers to 4% at lower Reynolds numbers. The higher turbulence could bring some fluid into the boundary-layer raising its capability to resist adverse pressure gradients, thus helping to delay flow separation.

The use of the alternative Reynolds number based on Thwaites method was not used here to replot the data of figures 8 and 9, because it did not bring any aditional information.

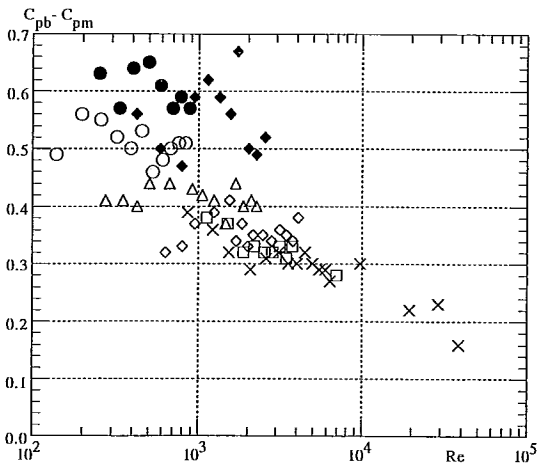

Figure 8 - Pressure rise coefficient for all solutions studied. □ 0.2% Tylose; ◊ 0.3% Tylose; Δ 0.4% Tylose; O 0.6% Tylose; ◆ 0.2% CMC; ● 0.4% CMC;X Newtonian.

5. CONCLUSIONS

Measurements of the vortex shedding frequency and form drag were carried out with various shear thinning weakly elastic polymer solutions and Newtonian fluids over a wide range of Reynolds numbers pertaining to the subcritical regime.

Pseudoplasticity was found responsible for reducing the boundary layer thickness over the cylinder and the shear layer thickness in the formation region, thus raising the maximum Strouhal number from the typical value of 0.2 for Newtonian fluids to about 0.24 for a power law index fluid of 0.56. Elastic fluids exhibited the opposite effect, because of the increased resistance of their molecules to be strongly deformed, thus thickening the boundary and shear layers.

An estimative of the real shear rates within the boundary layer over the cylinder was attempted following a procedure based on Thwaites integral method. The viscosity corresponding to this shear rate defined a new Reynolds number which provided less scatter of all the measured data than the use of a viscosity based on the free-stream velocity divided by the cylinder radius. Reynolds number effects associated with non-Newtonian fluids were also removed by this new definition of the characteristic viscosity.

The minimum form drag coefficient dropped by at most 15% when the power law index of weakly elastic Tylose solutions decreased from 1 to about 0.56. The elasticity further reduced the form drag coefficient so that with the 0.4% CMC solution the minimum C_d was of about 0.73, against a Newtonian value of 0.93. The observed behaviour of the CMC solutions agreed with results reported by other authors relative to flows around spheres.

The angle of flow separation decreased with the Reynolds number and was always higher than 90° for the non-Newtonian solutions. However, following the observed trend with Newtonian fluids at Reynolds numbers higher than those measured here, the separation is expected to occur on the forward half of the cylinder.

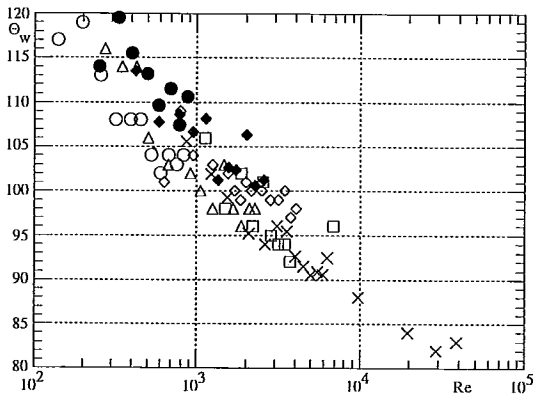

Figure 9 - Estimated wake angle for all solutions studied. □ 0.2% Tylose; ◊ 0.3% Tylose; Δ 0.4% Tylose; O 0.6% Tylose; ◆ 0.2% CMC; ● 0.4% CMC; X Newtonian.

ACKNOWLEDGMENTS

The authors wish to thank JNICT for the financial support through project PBIC/C/CEG/1370/92 and the equipment lent by INEGI and IDMEC. P. M. Coelho also wishes to thank the University of Porto for the leave of teaching duties over the last three years which made this work possible.

Finally, we gratefully acknowledge the helpfull comments of Prof. M. P. Escudier.

REFERENCES

Adachi, K., Yoshika, N. & Sakai, K 1977/78, An investigation of non-Newtonian flow past a sphere, J. Non-Newt. Fluid Mech., Vol. 3, pp 107-

Acharya, A., Mashelkar, R. A. & Ulbrecht, J. 1976 a), Flow of inelastic and viscoelastic fluids past a sphere. I Drag coefficient in creeping and boundary layer flows, Rheol. Acta, Vol. 15, pp 454-470

Acharya, A., Mashelkar, R. A. & Ulbrecht, J. 1976 b), Rheol. Acta, Vol. 15, pp 471-478

Achenbach, E. 1971, Influence of surface roughness on the cross-flow around a circular cylinder, J. Fluid Mech. Vol. 46, pp 321-335.

Bird, R. B., Armstrong, R. C. & Hassager, O. 1987, Dynamics of Polymeric Liquids. Volume 1: Fluid Mechanics, pp 1- 649, John Wiley & Sons.

Bloor, S. M. 1964, The transition to turbulence in the wake of a circular cylinder, J. Fluid Mech. Vol. 19, pp 290-304.

Cantwell, B. & Coles, D. 1983, An experimental study of entrainment and transport in turbulent near wake of a circular cylinder, J. Fluid Mech. Vol. 136, pp 321-374.

Durst, F., Melling, A. & Whitelaw, J. H. 1981, Principles and Practice of laser-Doppler Anemometer, Pergamon Press, London.

Escudier, M. P. 1996, Private communication on measurements of viscosity, oscillating material functions and first normal stress difference with CMC solutions, University of Liverpool

Farell, C., Carrasquel, S., Güven, O. & Patel, V. C. 1977, Effect of wind-tunnel on the flow past circular cylinders and cooling tower models, J. Fluids Engineering Vol 99, pp 470-479.

Gerich. D. & Eckelmann, H. 1982, Influence of end plates and free ends on the shedding frequency of circular cylinders, J. Fluid Mech. Vol. 122, pp 109-121.

Gerrard, J. H. 1966, The mechanics of the formation region of vortices behind bluff bodies, J. Fluid Mech. Vol. 25, pp 401-413.

Gerrard, J. H. 1978, The wakes of cylindrical bluff bodies at low Reynolds number, Phil. Trans. R. Soc. Lond. Ser. A, 288, pp 351-382.

Güven, O., Farrel, C. & Patel V. C. 1980, Surface-roughness effects on the mean flow past circular cylinders. J. Fluid Mech. Vol. 98, pp 673-701.

James, D. F. & Acosta, A. J. 1970, The laminar flow of dilute polymer solutions around circular cylinders, J. Fluid Mech. Vol. 42, pp 269-288.

James, D. F. & Gupta, O. P. 1971, Drag on circular cylinders in dilute polymer solutions, Chem. Engng. Prog. Symp. Ser. Vol. 67, 111 pp 62-73.

Maskell, E. C. 1963, A theory of blockage effects on bluff bodies and stalled wings in a closed wind tunnel, R. & M. N° 3400.

Metzner, A. B. & Astarita, G. 1967, External flow of viscoelastic materials: fluid property restrictions on the use of velocity-sensitive probes, AIChE J. Vol. 13, pp 550-555.

Norberg, C. 1994, An experimental investigation of the flow around a circular cylinder: influence of aspect ratio, J. Fluid Mech. Vol. 258, pp 287-316.

Oliveira, P. 1992. Computer modelling of multidimensional multiphase flow and application to T- junctions. PhD thesis. Imperial College, University of London, UK.

Pereira, A. S. & Pinho, F. T. 1994, Turbulent pipe flow characteristics of low molecular weight polymer solutions, J. Non-Newt. Fluid Mech. Vol. 55, pp 321-344.

Pinho, F. T. & Whitelaw, J. H. 1990, Flow of non-Newtonian fluids in a pipe, J. Non-Newt. Fluid Mech. Vol. 34, pp 129-144.

Pinho, F. T. & Whitelaw, J. H. 1991, Flow of non-Newtonian fluids over a confined baffle, J. Fluid Mech. Vol. 226, pp 475-496.

Roshko, A. 1961, Experiments on the flow past a circular cylinder at very high Reynolds number, J. Fluid Mech. Vol. 10, pp 345-356.

Stieglmeier, M. & Tropea, C. 1992, A miniaturized, mobile Laser-DopplerAnemometer, Applied optics, Vol. 111, pp 4096-4099

Serth, R. W. & Kiser, K. M. 1967, A solution of the two-dimensional boundary-layer equations for an Ostwald-deWaele fluid, Chem. Eng. Sci. Vol. 22, pp 945-956.

Shah, M. J., Petersen, E. E. & Acrivos, A. 1962, Heat transfer from a cylinder to a power-law non-Newtonian fluid, AIChE J. Vol. 8, pp 542-549.

Stäger, R. & Eckelmann, H. 1991, The effect of endplates on the shedding frequency of circular cylinders in the irregular range, Phys. Fluids A3 (9), pp 2116-2121.

Telionis, D. P., Gundappa, M. & Diller, T. E. 1992, On the organisation of flow & heat transfer in the near wake of a circular cylinder in steady and pulsed flow, Trans. A.S.M.E., J. Fluids Engng. Vol. 114, pp 348-355.

Tropea C. 1993 DFLDA Technical Reference Manual, INVENT GmbH, appendix B

West, G. S. &.Apelt, C. J. 1982, The effects of tunnel blockage and aspect ratio on the mean flow past a circular cylinder with Reynolds number between 10^4 and 10^5, J. Fluid Mech. Vol. 114, pp 361-377.

White, F. M. 1991, Viscous Fluid Flow, pp 1-614, McGraw-Hill, New York.